OPEN EUROPEAN JOURNAL ON VARIABLE STARS
June 2022 http://oejv.physics.muni.cz ISSN 1801-5964
DOI: 10.5817/OEJV2022-0231

A photometric study of the active EW/RS Binary Star System: GSC 05586-00371

BRINCAT, M. STEPHEN[1,6]; GALDIES, CHARLES[2,6]; GRECH, WINSTON[3]; TAVAKKOLI, FERESHTE[4]; HILLS, KEVIN [5,6]

1) Flarestar Observatory (MPC code: 171), Fl. 5/B, George Tayar Street, San Gwann, SGN 3160, Malta stephenbrincat@gmail.com
2) Institute of Earth Systems, University of Malta, Malta charles.galdies@um.edu.mt
3) Antares Observatory, 76/3, Kent Street, Fgura FGR 1555, Malta win.grech@gmail.com
4) University of Kashan, Kashan, Iran f.tavakkoli6889@gmail.com
5) Tacande Observatory, El Paso, La Palma, Spain kevinhills@me.com
6) American Association of Variable Star Observers (AAVSO)

Abstract: GSC 05586-00371 is a fast-rotating (Prot ≈ 0.44 days) eclipsing binary. Our study showed that this star system is an overcontact eclipsing binary star that belongs to the W UMa class with characteristics of RS CVn type stars. We studied this binary system by photometric means through the V and I bandpass where data by the ASAS-SN survey have also been utilized. our photometry yielded a more precise orbital period that was obtained on its discovery. ASAS-SN data over a 6-year period revealed a long-term photometric wave that is attributed to star spot activity. We monitored the binary system over a 73-hour monitoring period to detect any possible flares from the system, where two consecutive events were monitored from one of our observing stations. Through the use of the Wilson-Devinney program as applied by Binary Maker 3.0, we have obtained a model for this binary system that reveals the presence of star spots on both components. Our results show that the star spot activity is rather dynamic where their influence on the system's light output changed on seasonal timescales.

1 Introduction

In GSC 05586-00371 is a variable star that has been classified as an EW/RS binary star system. The W Ursae Majoris class that the star system belongs to, comprise around 95% of the known eclipsing binary variables. The W UMa components usually comprise two cool, main-sequence stars with spectral types ranging from F to K. These star systems orbit each other in proximity, which are close enough to exchange material from one another. Due to their proximity, W UMa stars have short orbital periods of less than a day with continuous light variation during their cycle, whilst the shape of the stars is warped in ellipsoidal spheres. This makes it hard to determine the exact times of the start and end of eclipses. The optical amplitude of this kind of variable star is usually less than 0.8 magnitudes through visual bandpass (Watson et al., 2010).

GSC 05586-00371 was recently discovered to be a variable source on 30th October 2016 from Flarestar Observatory through time-series photometry. The light curve acquired showed the characteristic light curve morphology of a W UMa variable star, however, RS

DOI: 10.5817/OEJV2022-0231

Canum Venaticorum (RS CVn) traits were also identified, and thus GSC 05586-00371 was classified as an EW/RS class star system.

The study of binary star systems has always been regarded as an important field in the study of stellar astrophysics as these star systems give an insight on the absolute sizes of the stars that are crucial for the calibration of the basic framework of astrophysical relations (Monesinos et al.,1998).

W UMa star systems are contact binaries where both components are embedded within a common envelope that covers the spatial extent in between the inner and outer Langrangian point with equipotential surfaces. A classification scheme devised by Binnendijk (1965) exhibits light curves of W UMa star systems that have a deeper minimum that occurs due to the occultation of the secondary star that has a lesser mass than that of the primary star. The other sub-class comprises the A-type systems where stars are of earlier spectral type than those of the W UMa counterparts and appear to have evolved further (Mochnacki, 1981).

The traits identified for RS Canum Venaticorum were originally attributed to starspots as explained by Skumanich (1972) that result from its fast rotation but which later studies suggested being from a strong correlation between magnetic activity, stellar rotational velocities and periods. Tidally locked binary stars such as W UMa stars are also known to exhibit strong magnetic activity. W UMa stars have also been found to show brightness variations due to starspots (Mullan, 1975) and hence W UMa systems have also some relation to the RS CVn class.

A number of RS CVn binaries with orbital periods between 1 and 14 days have been defined by Hall (1976) as stars that exhibit prominent H and K emission in the spectrum when observed whenever these stars were not undergoing an eclipse. For those with periods longer than 14 days, they were classified as part of the long period group. Some of the RS CVn stars are known to be eclipsing binaries that exhibit interesting photometric variations that are likely to be caused by chromospheric activity cycles lasting a number of years (Buccini & Mauas, 2009). RS CVn stars are usually composed of F-K type dwarf or giant stars with short duration orbital periods and which exhibit strong magnetic activity likely due to rapid rotation of one of the components.

The observation of single star systems is important to understand the underlying mechanisms of stellar activity that are not only of high scientific value to the stellar community but may also be important to exoplanet investigations as the presence of starspots can induce quasi-periodic frequencies in the light curves over a range of timescales from weeks to years (Barros et al., 2014). In this paper we examined the stellar activity of the GSC 05586-00371 system through surface brightness variations inhomogeneities that originate from the total flux, amplitude, frequency and phase.

As GSC 05586-00371 also belongs to the W Ursa Majoris (W UMa) class system, an investigation of such systems is important in the context of recording any orbital decay due to magnetic braking emanating from orbital angular momentum loss (Li et al., 2004)

DOI: 10.5817/OEJV2022-0231

2 Discovery of GSC 05586-00371

The phenomenological characteristics of the acquired light curve revealed that GSC 05586-00371 is a binary system that undergoes continuous partial eclipses over a period of 0.441456 days. This discovery was made after merging data from the "All Sky Automated Survey" ASAS-3 (Pojmański et al., 2001), "Catalina Real-time Transient Survey" CRTS (Djorgovski et al., 2011), "Northern Sky Variability Survey" NSVS (Woźniak et al., 2004); "AAVSO Photometric All Sky Survey" APASS (Henden et al., 2016) with data derived by Brincat S.M. (fig. 1) The star's brightness varied between a magnitude range of 13.4 to 13.8v through the V Johnson bandpass. A distortion wave within the light curve was identified that is typical amongst RS CVn stars. The AAVSO International Variable Star Index (Watson et al., 2010) confirmed this discovery as a new variable star on 2016 Nov 01 and was assigned an AAVSO Unique Identifier AUID 000-BMC-748.

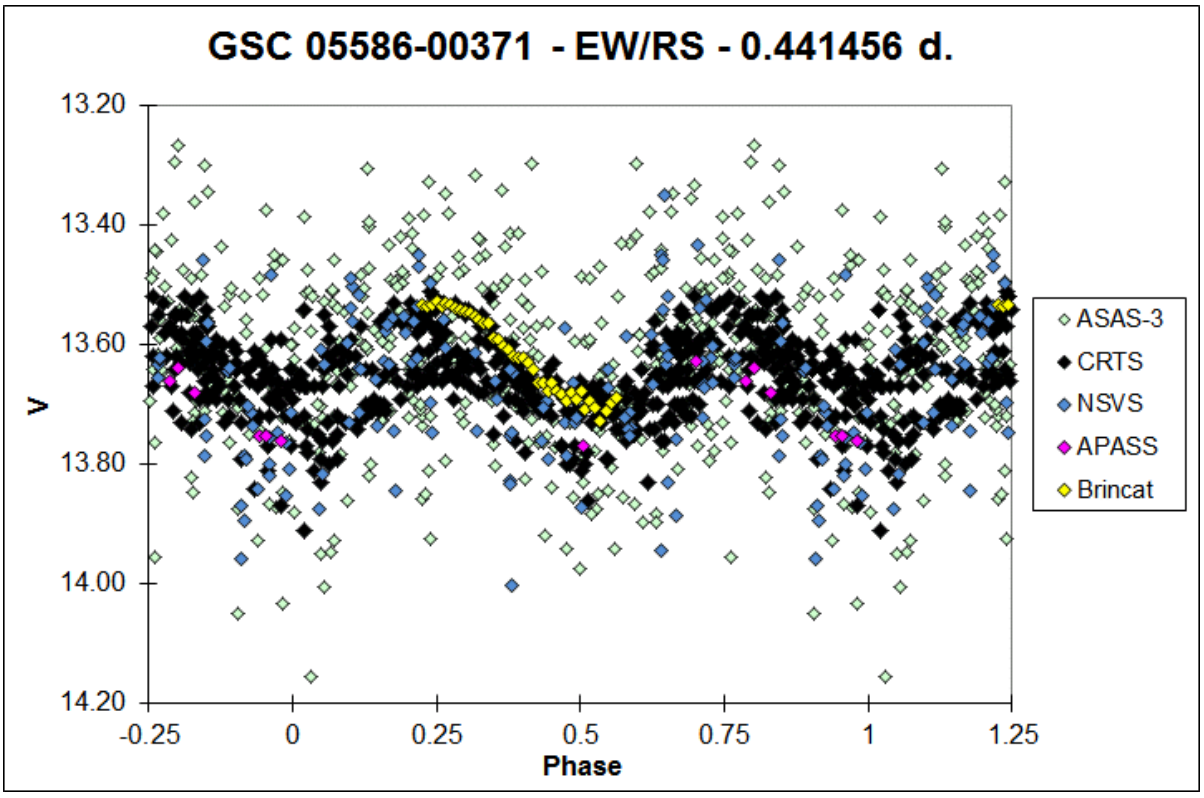

Figure 1: A Composite phased lightcurve showing the correct period. Scatter in data is due to star-spots on one of the stars.

The discovery that GSC 05586-00371 pertains to the EW/RS class (Watson et al. 2010) prompted this study to further investigate this star in more detail. An observational campaign led by the observatories shown in Tab. 1 was initiated to derive more information, including its stellar characteristics.

DOI: 10.5817/OEJV2022-0231

Table 1: Equipment and observatories details. CCD cameras were operated at sensor temperature ranging from -20˚ to -15˚ C.

Observatory / (Location)	Observer	Telescope	Filters	CCD Sensor	FoV (arcmin)/Binning	Pixel Scale (arcsec/pixel)
Tacande Observatory (La Palma, Spain)	Hills K.	0.500-m Optimised Dall Kirkham	B, V	FLI ML3200/ KAF3200ME	35.7 x 24.1 / 1x1	0.98
Antares Observatory (Fgura, Malta)	Grech W.	0.279-m SCT	C	SBIG STL-11000/ KAI-11000M	45.9 x 30.6 /2x2	1.37
Flarestar Observatory (San Gwann, Malta)	Brincat S.M.	0.254-m SCT	V, Ic	Moravian G2-1600 / KAF 1603ME	25.5 x 17.0 / 1x1	0.99
Znith Observatory (Naxxar, Malta)	Galdies C.	0.203-m SCT	V, Ic	Moravian G2-1600 / KAF 1603ME	30.0 x 20.0/1x1	1.17

GSC 05586-00371, also designated as UCAC4 388-064982, has been listed in several catalogs under other different designations. The GAIA DR2 catalog (Brown et al., 2018) designated the star's unique source identifier as '6312984381838649088'. The GAIA DR2 catalog has listed this star as having a stellar effective temperature of 5483 K with a distance of 907.11 pc with a higher and lower bound of a confidence interval of 955.01 and 863.71 pc respectively. The Gaia DR2 regression results by Bai et al. (2019) for GSC 05586-00371 yielded an effective temperature of 5693 K ±110 K. This value matches star characteristics belonging to spectral class ~G4V (Pecaut and Mamajek 2013), which makes the total light from these components having solar-color and convective atmospheres. Such characteristics point to a dwarf, low-temperature binary system.

GSC 05586-00371 has also been detected by the GALEX UV Satellite where GALEX data GR6+7 reveals the presence of ultraviolet light that is typical of many RS CVn systems. The GALEX/NUV calibrated AB magnitude by DR6+7 shows a NUV reading of 18.776 ± 0.0776 (Bianchi et al., 2017). The UV excess is thought to be due to free-emission of very hot plasma (~106 K) plasma (Rhombs & Fix, 1976) from its chromosphere.

3 Observations

GSC 05586-00371 was observed through the Johnson B (4361 λeff., 890 Δλ), V (5448 $\lambda_{eff.}$, 840 Δλ) and Cousins I (7980 $\lambda_{eff.}$, 1540 Δλ) bandpass using the instruments listed in Tab. 1. The system was also observed through a Clear-filter, based on the V-magnitude standard where such observations have been reported as CV magnitudes. All our brightness measurements were derived through differential aperture photometry with zero-points

DOI: 10.5817/OEJV2022-0231

calibrated to the APASS Catalog (Henden et al., 2016). All images obtained were calibrated through dark frame and flat field subtraction. The field location of GSC 05586-0037, comparison stars, and check star used are shown in Fig. 2 and Tab. 2.

Images obtained from Flarestar, Znith, and Antares Observatories utilized a minimum exposure length of 180 seconds, to gain enough signal to minimize scatter in our light curve. Tacande Observatory's contribution utilized 40-second exposures throughout our campaign. Nearly all our observations were carried out when the observation target was equal to or higher than 30^{o} above the local horizon.

Table 2: Source of comparison stars for GSC 05586-00371 based on APASS (Sequence X25410AJJ) magnitudes and GAIA DR2 positions. ‘C1’ and ‘C2’ are comparison stars while ‘K’ was utilized as a check star.

Star	RA	Dec	Label	B	V	I	(B-V)
GSC 05586-00371	14 55	-12 30	Variable	14.416	13.705	12.302	0.710
(V*)	43.26	28.5	Star	(0.078)	(0.06)	(0.074)	
GSC 05587-00174	14 56	-12 30	131	13.738	13.119	12.227	0.619
(C1*)	20.44	15.7		(0.038)	(0.022)	(0.101)	
GSC 05586-00377	14 55	-12 31	137	14.415	13.680	12.745	0.735
(C2*)	52.78	15.3		(0.072)	(0.032)	(0.079)	
GSC 05586-00411	14 55	-12 31	135	14.405	13.481	12.353	0.924
(K*)	59.73	52.9		(0.062)	(0.040)	(0.109)	

Observations of GSC 05586-00371 were acquired between the period of 30th October 2016 at the time of discovery up to 08 April 2021 through the Johnson B and V and Cousins I bandpass. Several observations through a clear filter based on a V bandpass framework have been acquired which are now reported as CV magnitudes. An offset has been applied to all CV observations to conform with the V-bandpass.

DOI: 10.5817/OEJV2022-0231

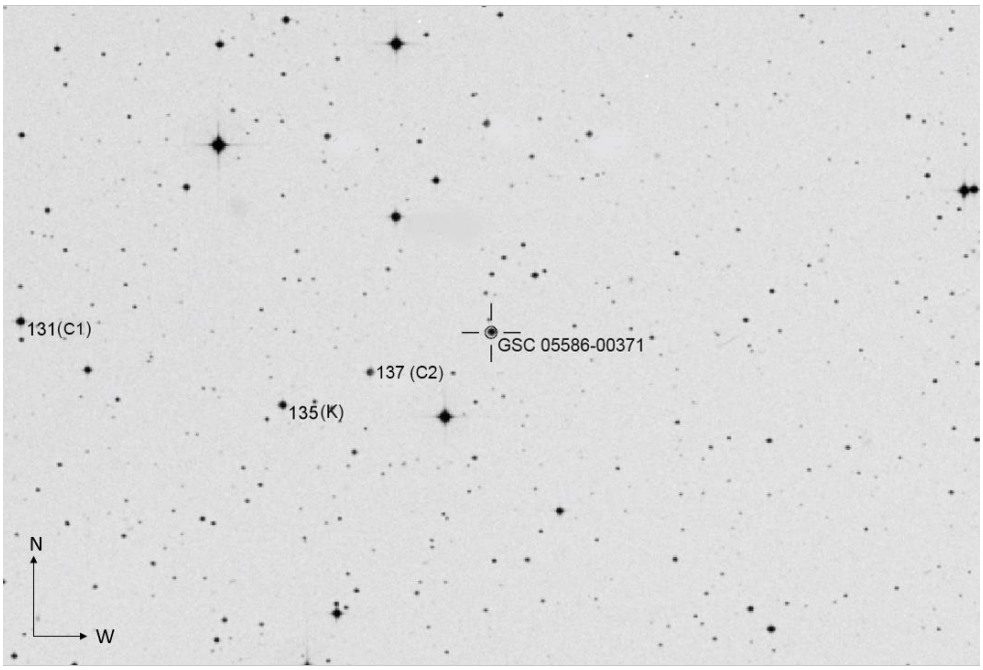

Figure 2: A Field location of the Variable Star (GSC 05586-00371) that harbors in the constellation of Libra. Comparison Stars (122, 131) and Check star (135) were used in this study. The field covers an area of 12' × 18'.

For the detection of short-term chromospheric activity such as flaring events, we have utilized all the available bandpass as obtained from each observatory. Our orbital period investigation has been carried out through B, V, and I bandpass.

3.1 Color Index

We have measured the color index (V–I) of GSC 05586-00371 as 0.868 ± 0.030, using the values of the magnitudes at the minima through V and Ic light curves as determined with a 4th-order polynomial fit in Peranso (Paunzen & Vanmunster, 2016). A de-reddened color index was obtained using the NASA/IPAC Extragalactic Database - Coordinate Transformation and Galactic Extinction Calculator (NASA/IED, 2015). The total galactic visual extinction was calculated along the line of sight at the coordinates of GSC 05586-0037. The color excess is shown in equations I and II.

$$E(B–V) = AB – Av = 0.282 – 0.213 = 0.069 \quad \text{(I)}$$

and

$$E(V–I) = Av– AI = 0.213 – 0.117 = 0.096 \quad \text{(II)}$$

Using the derived (V–I) color index and assuming an error of 0.02 for Av and Ar as described in Schlafly and Finkbeiner (2011), we have calculated the de-reddened color index for GSC 05586-00371 as:

DOI: 10.5817/OEJV2022-0231

$$(V–I)Min = (V–I) – E(V–I) = (0.890 – 0.096) \pm 0.03 = 0.794 \pm 0.03$$

$$(V–I)Max = (V–I) – E(V–I) = (0.870 – 0.096) \pm 0.03 = 0.774 \pm 0.03$$

According to Mamajek (2019), the average color index (derived from the average color index (CI) at maximum and minimum as 0.784) of (V–I) fits with spectral type G8 V with an effective temperature of ~5490 K.

3.2 Times of Minima

Since the discovery of GSC 05586-00371, we have acquired the Times of Minima (ToM) shown in Tab. 3. Entries are self-explanatory with the source header including the time of minimum in HJD, observatory and 'Type' which refers to whether the eclipse observed was of the primary (I) or secondary (II) eclipse. The computed error of our ToM is also included following the Cycle Number and Observed minus Calculated (O-C) residual.

We have used Minima software (Ver. 2.3) by Nelson (2006), to employ the algorithms below. Our results have been derived through a weighted mean including the standard deviation of means. To determine the Time of Minimum (ToM), we have used the following algorithms: Parabolic fit; Kwee and van Woerden; Fourier Fit, sliding integrations, and the Tracing Method where results were computed through a weighted mean (see Tab. 3).

The O-C diagram shows a possible downward trend, however, due to the limited number of observations, it is uncertain whether the O-C residual of GSC 05586-00371 is indeed decreasing.

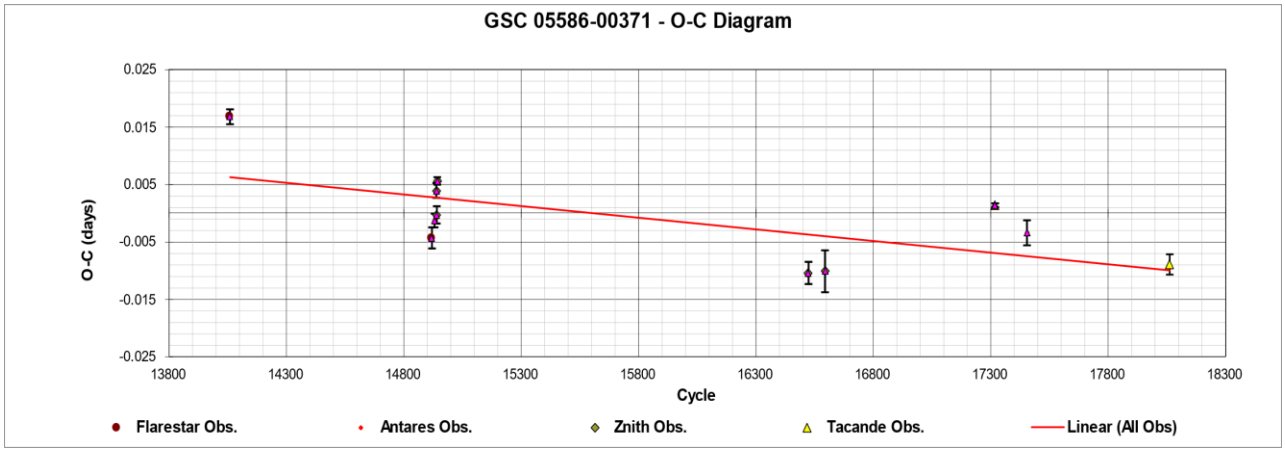

Figure 3: Observed minus Calculated (O-C) curve for GSC 05586-00371 based on observations shown in Table 2 and fitted through a polynomial based on the 2nd Order.

DOI: 10.5817/OEJV2022-0231

Table 3: Times of Minima including Observed minus Calculated residuals.

Session N.	Observatory	Type	ToM	Error	n'	n	O-C	Lin Fit	Date (DD/MM/YYYY)
S0089	Flarestar	I	57513.61344	0.0013	14059.53807	14059.5	0.016808	0.001784227	05/05/2016
S0184	Flarestar	I	57893.46524	0.00183	14919.9903	14920	-0.00428	-7.84024E-05	19/05/2017
S0187	Antares	I	57898.32429	0.00119	14930.99718	14931	-0.001246	-0.000102213	24/05/2017
S0190	Znith	I	57901.41972	0.00129	14938.00904	14938	0.003992	-0.000117365	27/05/2017
S0197	Znith	I	57902.5191	0.00151	14940.49939	14940.5	-0.000268	-0.000122776	29/05/2017
S0187	Znith	I	57903.40793	0.00065	14942.5128	14942.5	0.00565	-0.000127106	29/05/2017
S0825	Znith	I	58601.55456	0.00193	16523.97648	16524	-0.010384	-0.003550404	28/04/2019
S0835	Znith	I	58632.45677	0.00364	16593.97713	16594	-0.010094	-0.003701926	28/05/2019
S1107	Tacande	I	58952.52388	0.00033	17319.00321	17319	0.001416	-0.000687948	13/04/2020
S1154	Antares	I	59012.33633	0.00218	17454.49225	17454.5	-0.003422	-0.005564555	11/06/2020
S1246	Tacande	I	59280.7361	0.00177	18062.47984	18062.5	-0.0089	-0.007644407	06/03/2021

The previously published linear ephemeris formula (III) has been updated based on the observations (see Tab. 3) that are reflected in the IV elements shown below, with a combined uncertainty of 0.006 (using the RSS method), an expansion coefficient (k) of 2.0 and uncertainty of 0.012.

$$\text{HJD } 2451306.946 + 0.441456\ d \times E \qquad \text{(III)}$$

$$\text{HJD } 24559280.51663288 \pm 0.0001 + 0.441453554 \pm 0.012\ d \times E \qquad \text{(IV)}$$

OPEN EUROPEAN JOURNAL ON VARIABLE STARS
http://oejv.physics.muni.cz
DOI: 10.5817/OEJV2022-0231
ISSN 1801-5964

4 Photometry

Extensive photometric coverage of GSC 05586-00371 was obtained during the period 2017 and 2020. A change in the morphological features of the light curve has been attributed to the change of brightness variation arising from the O'Connell effect (O'Connell, 1951) as a possible indicator of spot activity where a difference in brightness between the two maxima has been observed.

Fig. 4 shows the light curve of GSC 05586-00371 as obtained during an observation campaign. Observations for this lightcurve were acquired through a clear filter and adjusted to V band, designated as CV (Clear to V) bandpass. This lightcurve that was obtained in 2017 shows a difference in maxima as recorded through clear-filtered observations.

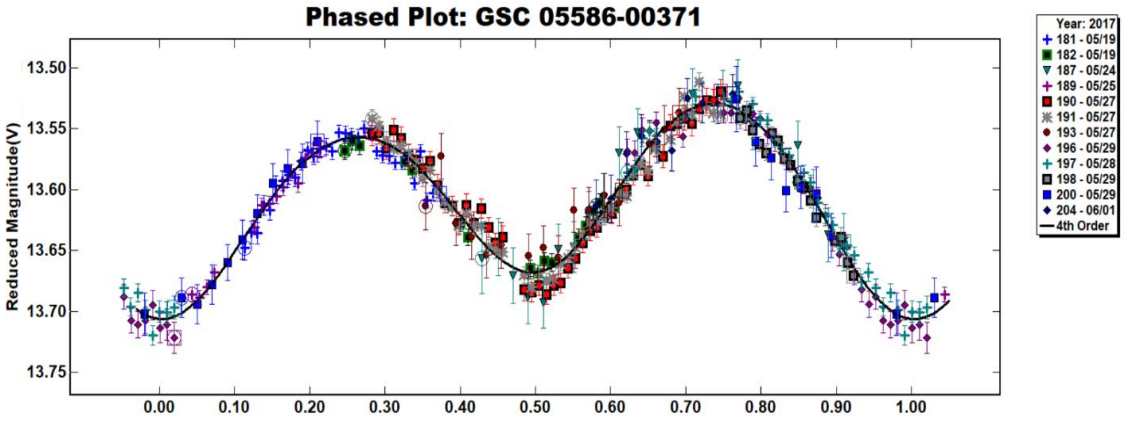

Figure 4: Lightcurve of GSC 05586-00371 as obtained through a Clear filter (CV). These observations were obtained to obtain the time of minimum and for the detection of any possible flares. Note that the characteristic of the O'Connell effect is clearly depicted through an asymmetry in the maxima of the phased light curve.

Colorimetric data was also obtained from our observatories around May 2017 through V and I bandpass (Fig. 5). The derived light curve shows a continuous sinusoidal curve where the trough of the first phase at 0.25 shows a lower maximum brightness than that of the second sinusoidal wave. It is at this point that the brightness difference between the maxima in the light curves is attributed to the O'Connell effect. The attenuation of the first phase has been likely caused by a group of stellar spots or a large stellar spot that has or have attenuated the light from the primary star (brightest) star in the system. This feature can also be indicative of the presence of stellar spots on one or both of its stars. The light curve also shows that there is a subtle difference between the depth of the primary and secondary eclipse, suggesting that both stars have similar temperatures, with the secondary member having a cooler photospheric temperature than the primary star. The amplitude depths of the primary minimum in our light curve are 0.195 ± 0.015 and 0.165 ± 0.05 mag in V and I

OPEN EUROPEAN JOURNAL ON VARIABLE STARS
June 2022 http://oejv.physics.muni.cz ISSN 1801-5964
DOI: 10.5817/OEJV2022-0231

Lightcurve of GSC 05586-00371 as acquired during 2017 and 2020

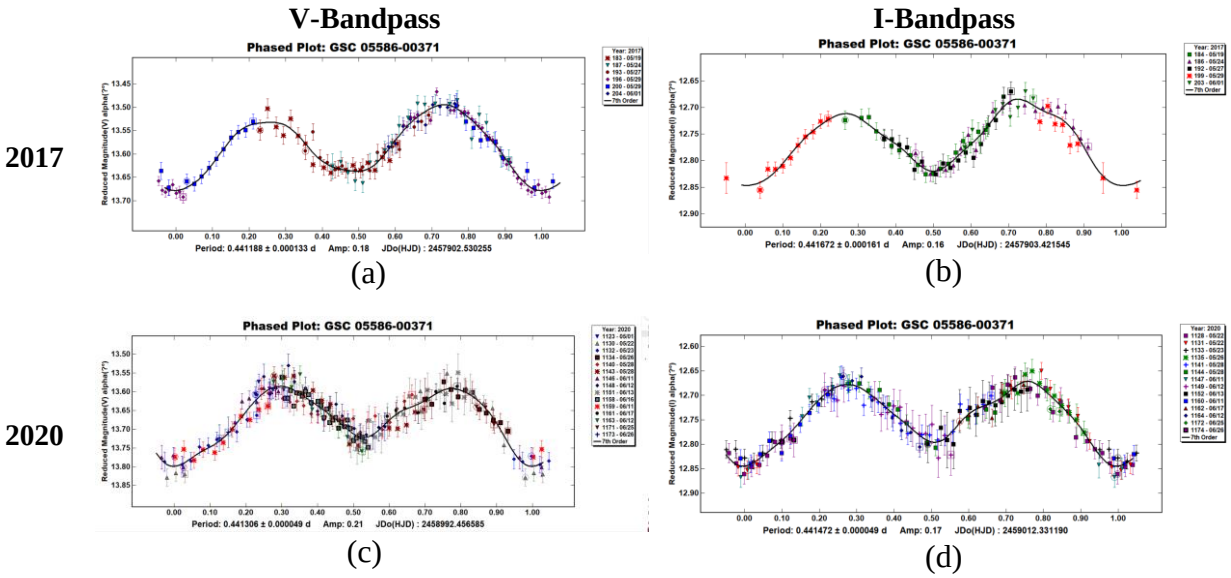

Figure 5a-d: Lightcurves of GSC 055586-00371 acquired by this study during the 2017 and 2020 through V and I bandpass. The difference in between the maximum brightness (phase 0.25) between the 3 years is visible indicating an evolutionary stellar spot cycle. Data points indicate the start (circled) and end (squared) of the respective nightly observation.

passband respectively (Fig. 5). The secondary minimum of GSC 055586-00371 has exhibited an amplitude depth of 0.0625 ± 0.0175 and 0.04 ± 0.025 mag in the V and I passbands respectively.

The 2017 data (Fig. 5a) shows a light curve with unequal maxima; however, more recent observations show that the difference between the two maxima has nearly disappeared in 2020, indicating a probable dissipation of the stellar spot or stellar spot group on the primary star.

On the other hand, the 2020 light curves (Fig. 5 c and d) show that the brightness of the maxima at phase 0.25 has increased when compared with the 2017 light curve. The total brightness of this phase became nearly identical to the maxima at phase 0.75. This could imply that during the 2020 observation period of 57 days, the spot/s visible through this phase have attenuated to levels below our detection thresholds. As GSC 05586-00371 exhibit RS CVn characteristics, some variation can be expected from one observation season to the next but the significant decline of spot presence was rather unexpected. Such dynamicity makes this system more active than anticipated.

Another significant change was also observed in the total light output of the star system for the period 2017 and 2020, during which an observed brightness decline of maximum light of 0.04 mag (v) and 0.02 mag (Ic) magnitudes and a decrease of 0.1 mag (v) and 0.06 mag (Ic) at primary minimum were noted. (see Fig. 6). This results in a total amplitude increase

of the system from 0.18 to 0.21 magnitudes in the V passband and 0.15 to 0.17 magnitudes in the Ic passband.

4.1 Long-term variability

In consideration that GSC 05586-00371 shows photometric characteristics belonging to RS CVn class, we have further investigated whether this stellar system exhibits long-term variation in its total flux using the "All Sky Automated Survey for Supernovae" (ASAS-SN; Kochanek et al. 2017) data.

To investigate the long-term variation this long-term variability is usually caused by stellar spots on the photosphere on a member (or even both members) of a binary system (Steenwyk et. al., 2013) on a time frame lasting a number of years (Buccino and Mauas, 2009), we have obtained ASASSN observations obtained through the Johnson V and the Sloan g' bandpass for the period JD 2455985.1408 to JD 2459109.2246. This covered a period of 3124 days (8.55 years). To gain a normalized lightcurve, an offset to the g' bandpass data was applied to align with the V bandpass baseline data by -0.28526. Fig. 7 shows the normalized lightcurve that depicts the V (green) and g' (purple) bandpass ASASSN observations.

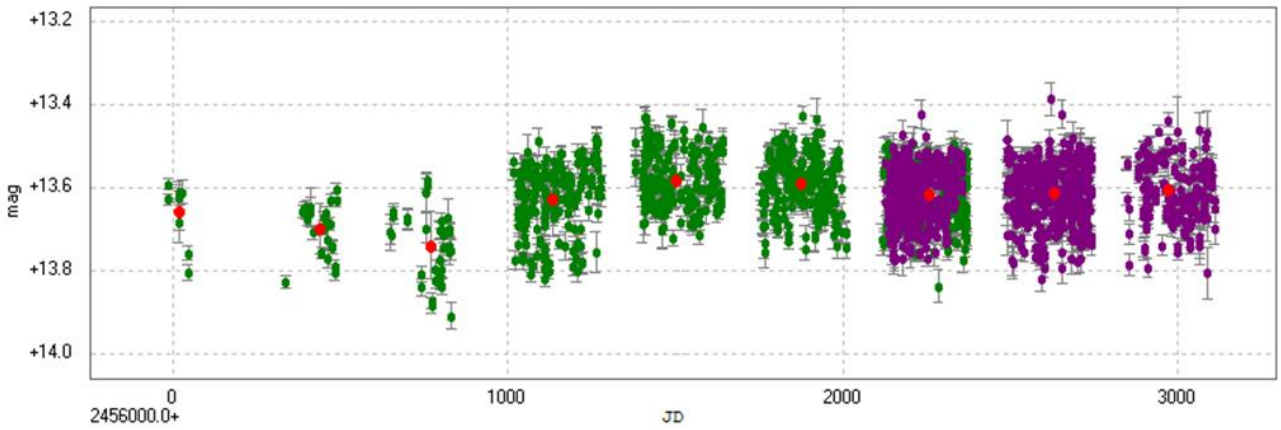

Figure 6: Lightcurve showing the combined 'V' and g' ASAS-SN datasets, where an offset has been applied to g' data. V-bandpass is green; g' band is purple. The red points in each seasonal dataset represent the average mean magnitude of the cluster.

For the ASASSN dataset included in Fig. 6, a routine period search was conducted using the Phase Dispersion Minimization (PDM) technique (Stellingwerf, 1978) for long period variation over long time scales of years analogous to the solar cycle. This technique was

DOI: 10.5817/OEJV2022-0231

applied for other period search algorithms in view that the PDM is suitable to search for periodicities whenever limited observations are available. Using this technique, the present results show two possible long-term periods of 2845 ± 593 d and 3164 ± 396 d, with the latter having the best residuals.

Through the use of the data in Tab. 4, we elaborated further the likely long-period cycle of GSC 05586-00371 as 3164 ± 396.57 days with an amplitude of 0.116 magnitudes. This variation can be explained by the fact that RS CVn systems normally constitute late-type giants or subgiants where a significant level of activity is observed having similar behavior to our Sun. The presence of cooler darker spots can alter the resultant light curve of the star's brightness through rotational modulation with brightness variation ranging from several hundredths to several tenths of a magnitude (Kozhevnikova & Alekseev, 2015). The smooth deviations from the recognized RS CVn light curves indicate slow changes of the spot configuration from season to season that affects the total brightness level of the system. Through colorimetric photometry, these deviations attributed to spot presence enables empirical determination of the temperature and combined area of the spots through lightcurve modeling. Fig. 7a shows the light curve based on the seasonal average and the resultant phased light curve from all of the ASASSN data based on the 3164-day (8.66 years) period (Fig. 7b). Within the limitations of our study, we have derived the periodogram based on seasonal data (see Fig. 7c), from which the phased lightcurve was derived. The phased lightcurve shows the best period fit of a 3164-day period (see Fig. 7d).

Table 4: Table 4. Averaged seasonal ASAS-SN data used in fig. 6..

Central JD of Season	Mean Magnitude	Error	Magnitude Standard Deviation
2456017	13.659	0.037301791	0.0746
2456438	13.698	0.029726394	0.0594
2456767	13.739	0.041032855	0.0821
2457134	13.628	0.044730711	0.0895
2457501	13.580	0.035494187	0.0710
2457876	13.591	0.033502044	0.0670
2458258	13.614	0.034977798	0.0700
2458629	13.611	0.036379714	0.0727
2458970	13.605	0.039019491	0.0780

http://oejv.physics.muni.cz
DOI: 10.5817/OEJV2022-0231
ISSN 1801-5964

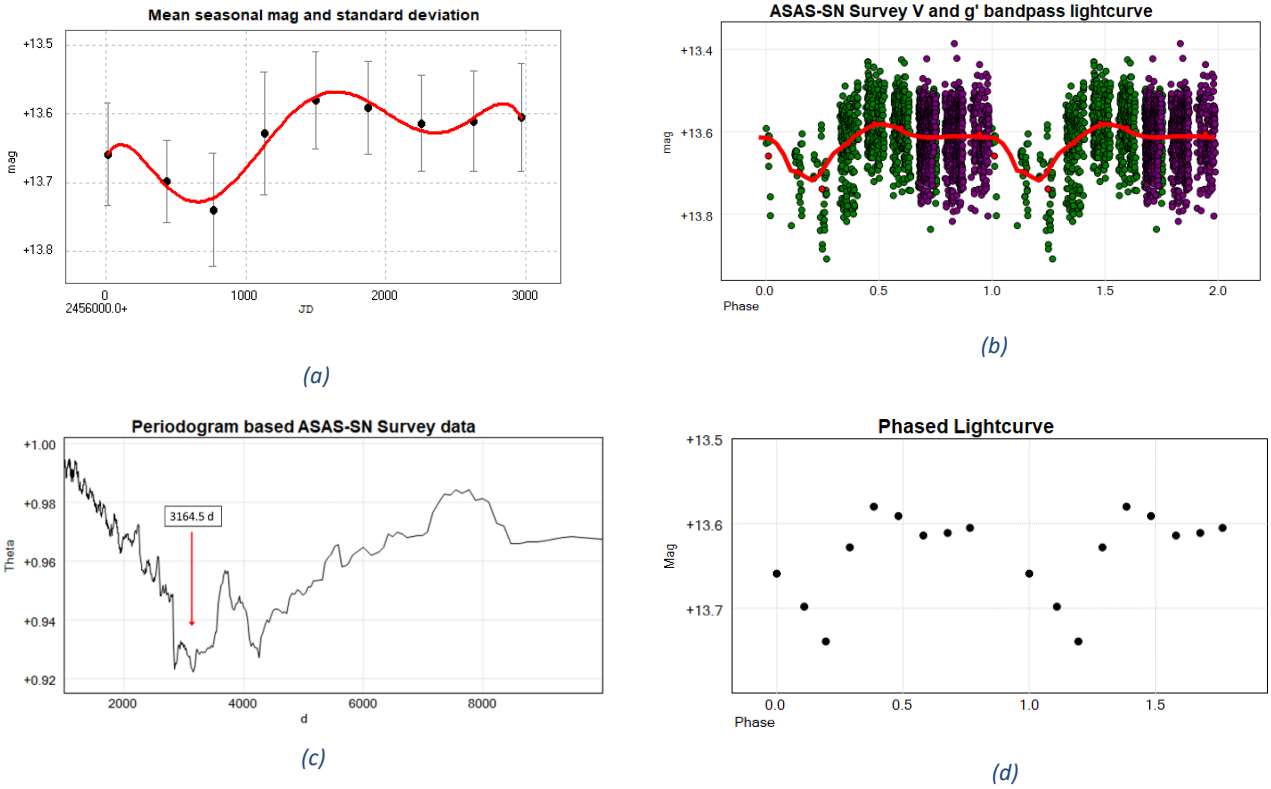

Figure 7a-d: Lightcurve of the mean magnitude for each season from 2012 to 2020. The Redline depicts polynomial fitting (6th order); (b) the phased lightcurve based on the (3164-day) or 8.66 years period; (c) the long-term periodogram results; (d) the phased lightcurve based on a period of 3164 days.

This long-term variation by GSC 05586-00371 is likely to be due to photospheric activity that brings about a higher incidence of stellar spots over the star's disk. This is likely to be due to either a number of small spots or fewer larger star spots on each of the star's photosphere (Steenwyk et. al., 2013) Models relating magnetic cycles to average brightness change have been developed that can account for up to around 0.1 magnitude variation in stars with high chromospheric activity (Hall, 1991).

4.2 Star Spot Activity

We hereby describe spot temperature and filling factor attributes based on the analysis of our photometric data. Contrary to the spots observed (via light curve synthesis) during the 2017 observations, our 2020 data covering the period May 01 to June 26 have shown an attenuation of spot presence. This implies that the spots observed are active on time scales of months or perhaps even weeks. Such transitory phenomenon of spot attenuation may have affected the activity of both stars through magnetic interaction as the spots derived from our 2020 data did not appear so pronounced as those during our 2017 observation run. On the 8

DOI: 10.5817/OEJV2022-0231

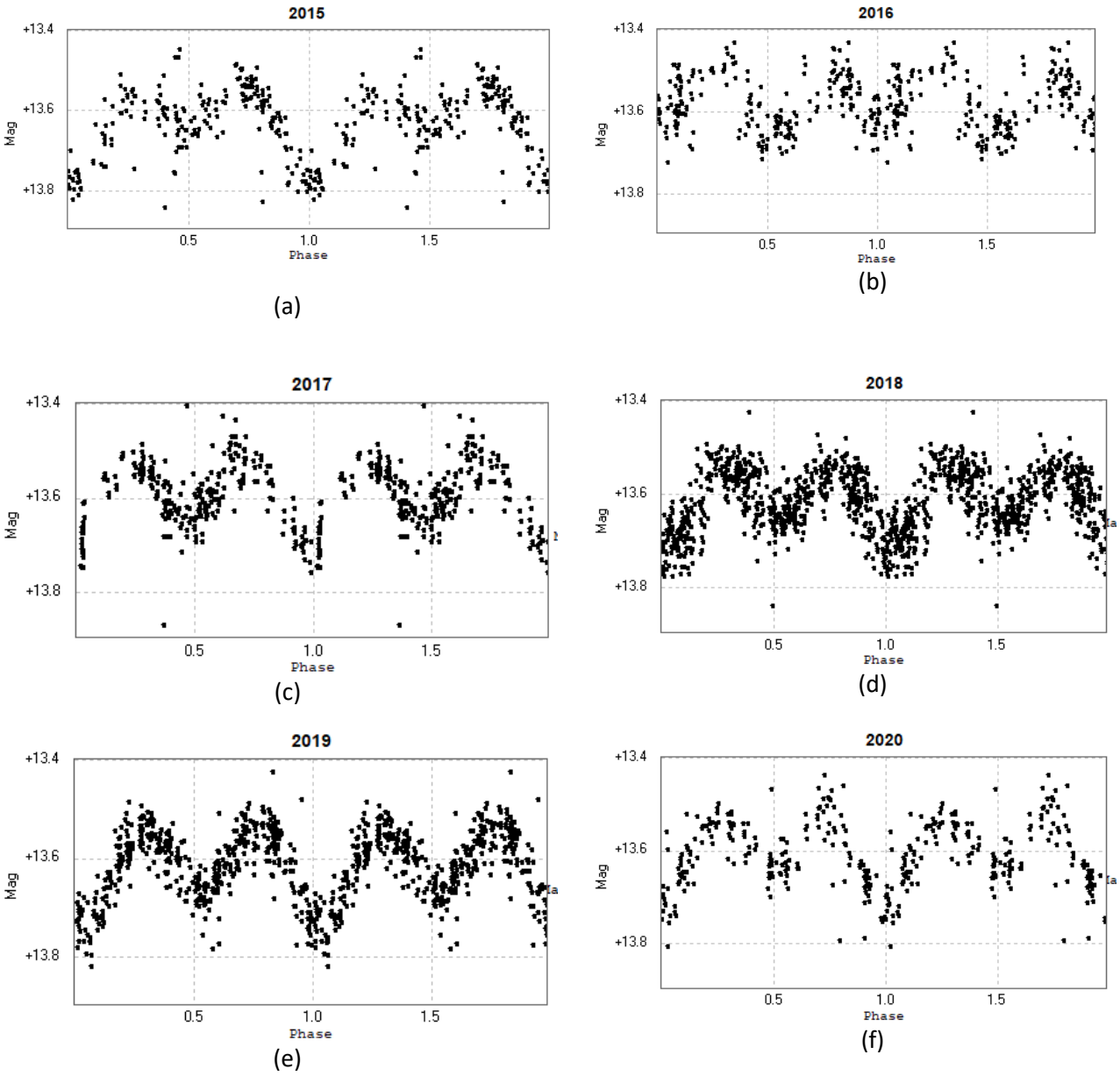

Figure 8a-f: GSC 05586-00371 ASASSN Datasets per yearly observation window.

other hand, the ASAS-SN data of the entire 2020 observation season do show the presence of spots via phase (0 to 0.5) attenuation, implying that spot activity on this system is quite dynamic.

Fig. 8a-f shows the data obtained by the ASAS-SN survey over a 6-year period. As previously mentioned, a long-term cyclic variation has been observed and this is reflected by the average brightness of the star at maximum and minimum. The ASAS-SN data also shows that 2016 has been a rather anomalous period as the amplitude of the average light intensity diminished significantly by around 0.05 magnitude. This indicates that during this period,

DOI: 10.5817/OEJV2022-0231

stellar spot activity deviated from the normal activity, and which led to a variation on the light curve morphology that was observed.

Interestingly, Fig. 8d-e also shows that during the years 2018 and 2019, the spots observed on the GSC 05586-00371 diminished to a point that both maxima of phases 0.25 and 0.75 were of equal intensity. This suggests that the spot observed on the primary star during 2015, 2017, and 2020 has contracted in size which has ultimately determined the total brightness of the primary wave.

Table 5: Monitoring for flaring events within the GSC 05586-00371 system.

Observatory	**Year**	**Nº of Obs. Sessions**	**Monitoring time (Hours)**
Antares	2020	17	41.66
Flarestar	2020	12	14.39
Tacande	2021	7	11.58
Znith	2020	5	5.49
		41	73.12

4.3 Short-Period Variations: Flares

Given that GSC 05586-00371 has been classified as a W UMa/RS CVn star based on the 2020 observation season, we attempted several monitoring sessions to detect any possible flares within the system similar to the W UMa star as reported by Qian et. al., (2014). On the basis of more than 3000 images, covering 73.12 hours of monitoring time acquired during the period 2020 May 26 to 2021 April 08, our new data shows 2 consecutive flaring events on the night of 2020 July 15 (see Tab. 5). Due to the high noise level of the light curves, we applied a minimum threshold of at least 2 images per event in order to eliminate any possibilities of cosmic ray hits that might have affected the results of our differential photometry. In addition, a visual inspection of the images was carried out which ruled out any artifacts. A simple Image Grader Software (IGS) made available through our image acquisition software (Main Sequence Software, 2021) was also used to establish whether there was any telescope tracking or focus drift inconsistencies by using the Half Flux Radius (HFR) measurement on all of the images acquired during particular sessions. IGS uses a

OPEN EUROPEAN JOURNAL ON VARIABLE STARS
http://oejv.physics.muni.cz
DOI: 10.5817/OEJV2022-0231
ISSN 1801-5964

routine that performs focus quality analysis via relative grading metrics and is designed to calculate the HFR of all stars on a set of images where it grades each image according to the mean HFR output (Miyashita, 2007). Our HFR results did not reveal any anomalies during the session where flares were detected. Tab. 5 shows the monitoring times conducted through the instruments as per Tab. 1.

Table 6: Flaring events of GSC 005586-00371 as recorded by Antares Observatory.

Date/Session	Phase	Amplitude	Duration (Min:Sec)
20200715/S1191	0.11	0.17	12m38s
20200715/S1191	0.17	0.16	19m22s

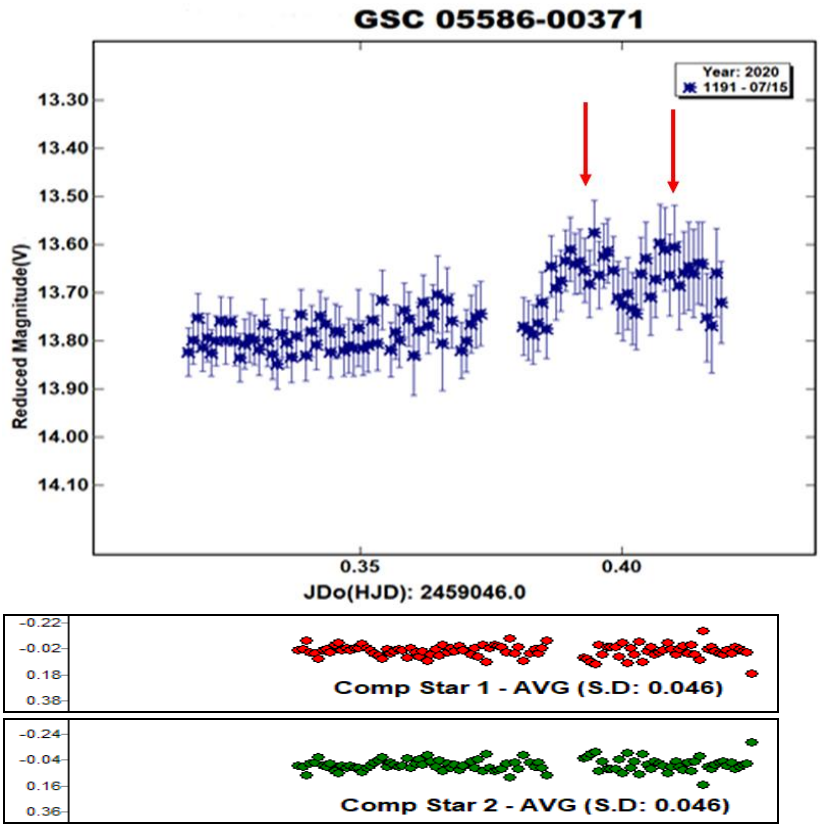

Figure 9: Lightcurve of the flaring events and comparison star residuals.

DOI: 10.5817/OEJV2022-0231

These two events were recorded at phases 0.11 and 0.17, where according to our binary star model as shown in the next section, corresponded to a time when the stellar spot/s on the primary star facing the Earth. The event with the highest amplitude was recorded on 2020 July 15 at 21:37 UT where we measured it to be of 0.17 mag (v) and with a duration of 19' 22''. Tab. 6 shows the details of flaring events detected on GSC 05586-00371. Fig. 9 shows the lightcurve and comparison star residuals further confirming the validity of this detection. Furthermore, we wish to note that a small number of additional suspected low-amplitude flares were detected, but due to their low intensity and noise levels of the light curves, it was not possible to derive results with high certainty.

4.4 Binary Star Model of GSC 05586-00371.

The V and Ic curves (based on 2017 and 2020 observation data) were modeled using Binary Maker 3.0 (Bradstreet and Steelman 2004). Our modeling results showed consistent fitting of data acquired through both filters. The derived model shows that GSC 05586-00371 is a shallow contact eclipsing binary with the following parameters: q=0.16 ± 0.01, fill-out=0.70 ± 0.05, i=46.0 ± 0.5, T1=5000 ± 50, T2=6300 ± 50, with one cool spot at each star at the respective location on the primary star Latitude 100.0 ± 5; Longitude 70 ± 5; and secondary star at Latitude 110.0 ± 5 and Longitude 110.0 ± 5. For our analysis, we utilized convective parameters of g=0.32, A=0.5.

The modeled star component temperature difference was estimated to be 1300 K. The solution was based on a framework of normalized fluxes through our V - Ic color data as shown in Fig. 5. Our derived parameters of GSC 05586-00371 system are defined in Tab. 6 above.

Due to the absence of any radial velocity data for this system, we employed known empirical relations obtained by other studies of several W UMa-type eclipsing binary systems. We used empirical relations derived from Terrell et al. (1992), as inputs in Binary Maker 3 Software (Bradstreet & Steelman, 2004) in addition to the following parameters: albedos (assumed 0.5 for both primary and secondary components for stars with convective envelopes of T < 7200 K; assumed gravity darkening coefficients of 0.32 for both components having convective envelopes, and limb darkening coefficients (through Van Hamme's table's interpolation). Moreover, it is highly plausible that the different depths of the minima in the light curve are due to the component's temperature differences.

Our derived model of GSC 05586-00371 depicts a varying photometric amplitude that was caused by a group of spots or by one spatially extensive spot on the primary and secondary component of the system where the spot temperature is cooler than the average photospheric temperature of the star concerned.

The observed light amplitude through the conversion of magnitude estimates to flux readings where due to the presence of dark spots facing the observer that has resulted in an observed decrease in brightness for the phases mentioned above. We have derived the spots

DOI: 10.5817/OEJV2022-0231

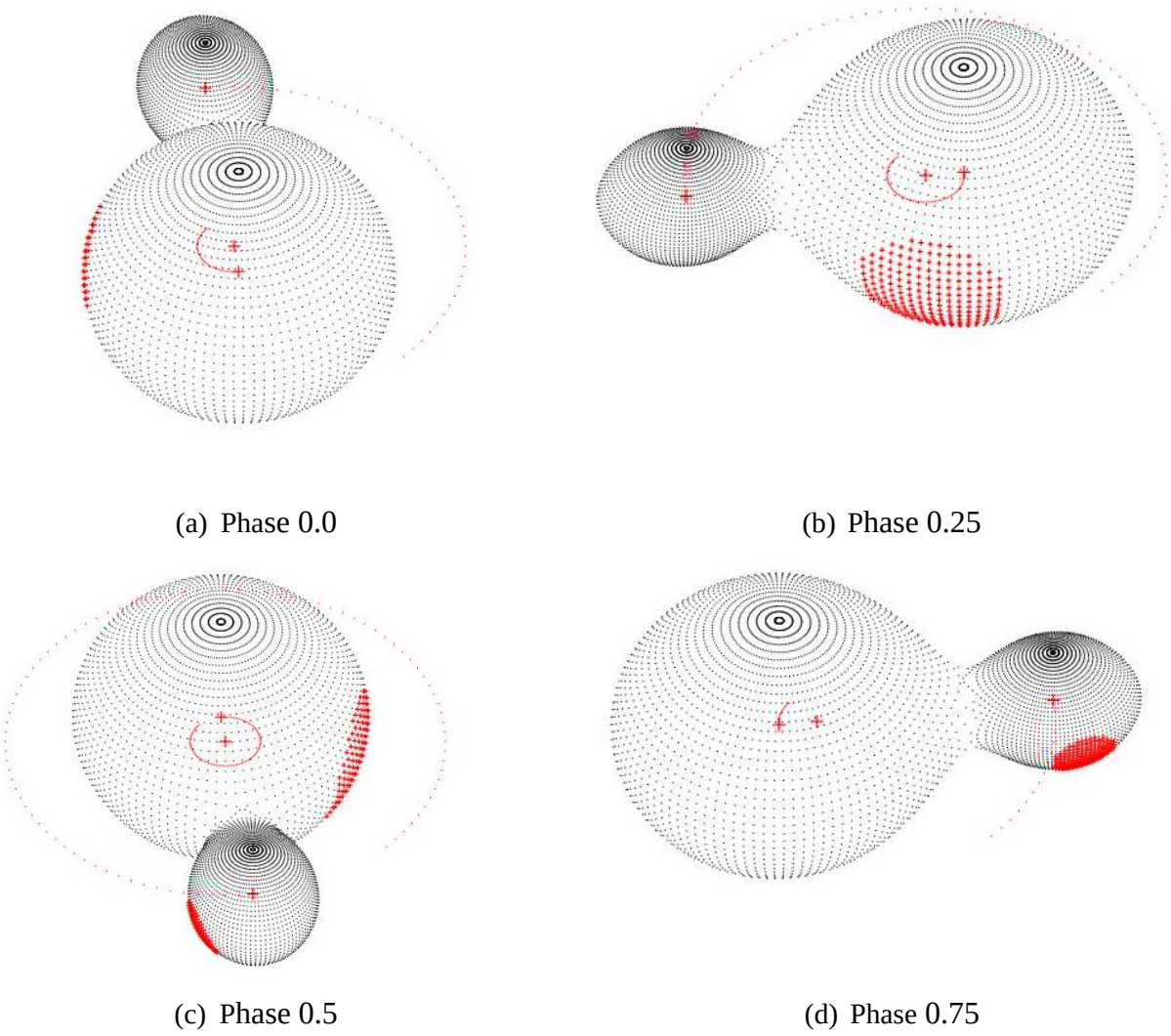

(a) Phase 0.0 (b) Phase 0.25

(c) Phase 0.5 (d) Phase 0.75

Figure 10a-d: Geometrical representation at various phases of the binary model of GSC 05586-00371 derived by Binary Maker.

by which spot temperatures were estimated through light curve modeling by the software that derives the estimated parameters of the spots via the morphological characteristics of the light curve. These results show a spot temperature on the primary component of ~2500 K, i.e.- half of its derived photospheric temperature of 5000 K. For the secondary star, we have also determined the spot temperature at 0.6 of the photospheric temperature at 6300 K, which is equivalent to a spot temperature of 3780 K. This data correlates well with our observed decreased Colour Index through the V and Ic bandpass.

Our derived model of the star system revealed that the best fit for the observed lightcurve of the location of the spot(s) on the primary star is at Colatitude of 100.0 ˚ ± 5 ˚ and Longitude of 70 ˚± 5 ˚(see Fig. 12a-d). The location of the star spot(s) on the secondary component at coordinates Colatitude of 110.0 ˚ ± 5 ˚ and Longitude of 27 ˚± 5 ˚.

DOI: 10.5817/OEJV2022-0231

Table 7: V, Ic, Wilson-Devinney program solution parameters of GSC 05586-00371.

Parameters	**Values**
λV, λI Wevelength (nm)	550, 790 nm
g1=g2 (gravity brightening exponent α)	0.32
A1=A2 (reflection coefficient)	0.5
Inclination (°)	46.0° ± 0.5°
T1, T2 Temperature (K)	5000 K ± 50 K, 6300 K ± 50 K
Ω	2.058 ± 0.001
q (m_2 /m_1)	0.16 M⊙± 0.10M⊙
Fill-outs (*f*): F_1, =F_2 (%)	0.70 %± 0.05 %
L_1 /(L_1+L_2 =1) I	0.6920 % ± 0.0002 %
L^1 /(L_1+L_2 =1) V	0.6058 % ± 0.0002 %
JDo (days)	2451306.946 ± 0.001
Period (days)	0.441 ± 0.012 d
R_1 / a, R_2/ a (pole)	0.522, 0.240
R_1 / a, R_2/ a (side)	0.580, 0.253
R_1 / a, R_2/ a (back)	0.607, 0.319

DOI: 10.5817/OEJV2022-0231

Table 7: continued

Parameters	**Values**
Spot 1, Star 1 (2017)	
Colatitude (˚)	100.0 ˚ ± 5
Longitude (˚)	70 ˚ ± 5
Radius (˚)	28.0 ˚ ± 0.5
T-Factor (Tspot/Tsurface)	0.50 ± 0.05
Spot 1, Star 2 (2017)	
Colatitude (˚)	110.0 ˚ ± 5
Longitude (˚)	110.0 ˚ ± 5
Radius (˚)	27.0 ˚ ± 0.5
T-Factor (Tspot/Tsurface)	0.60 ± 0.05

5 Conclusion

From the evidence collected, we infer that GSC 05586-00371 is an overcontact eclipsing binary star where both stars are in close proximity with each other that they are in contact with each other to share their gaseous envelopes. GSC 05586-00371 belongs to the W UMa class of variable stars with characteristics of RS CVn type stars. This study proposes that GSC 05586-00371 is a W-type subclass of W UMa variable stars as W-types exhibit a primary star that is physically larger, cooler, and more massive than its companion. The solar-like component stars revolve around each other over a period of 0.441 ± 0.012 days. As the system does not exhibit total eclipses and radial data was not available, the mass ratio - q, could not be determined with precision and thus some parameters have been derived through empirical results obtained for other similar star systems. Our photometric results allowed us to derive the temperatures of each component and adopt the temperature difference for our modeling. Furthermore, we have established most of our parameters

through the fitting of our light curves through V and Ic bandpass that permitted us to build a system model through the Wilson-Devinney program as provided by Binary Maker 3.0.

In consideration that the temperature difference between the two components of GSC 05586-00371 is around 1300 K, we believe that GSC 05586-00371 can be termed as a young poor thermal overcontact binary star system where the stars have not been in contact for long enough time to reach thermal equilibrium (Csizmadia & Klagyivic, 2004).

Regarding the long-term variation of this system due to star spot evolution, that is a characteristic of RS CVn stars, this study has had only a limited temporal coverage at its disposal. The data at hand did not cover the whole of the derived long-term period of 3164 days (8.65 years) that had an amplitude of 0.116 magnitudes and thus we are unable to derive any long-period estimate with any certainty.

On the basis of the observations deemed to be consistent with possible flaring events, and in view that W UMa systems can exhibit such events, an extended monitoring campaign was initiated to systematically record any possible flaring events. The resulting 73-hour observational campaign yielded two candidate flaring events that were recorded consecutively on the night of 2020 July 15 from Antares Observatory. Our analysis of this session did not reveal any anomalies. Hence, we have reasons to believe that the flaring events recorded are real and thus this makes the GSC 05586-00371 star system more dynamic than envisaged. However, it is being recommended that enhanced techniques can be used further to recover more possible flaring events.

Satellite missions that monitor the sky on a regular basis such as the TESS and GAIA missions might shed more light on the activity of GSC 05586-00371. This is even more interesting from the point of view of exoplanet habitability, where a growing number of exoplanets are being discovered around binary stars.

The binary star model derived by this study depicts a system that is typical to W UMa stars and the presence of starspots reminiscent of RS CVn systems have made the system more photometrically dynamic and interesting to follow.

The acquisition of radial velocities of this binary system would be highly desirable in order to obtain absolute system parameters instead of the relative parameters used here. Further investigation to shed more light on this interesting binary star system is highly recommended.

Acknowledgements: This research has made use of the AAVSO Photometric All-Sky Survey (APASS), funded by the Robert Martin Ayers Sciences Fund and NSF AST-1412587.

References

Bai, Y., et al. 2019, AJ, 158, 93, 2019AJ....158...93B
Barros, S. C. C., et al. 2014, A&A, 569, A74, 2014A&A...569A..74B

Binnendijk, L. 1965, in The Position of Variable Stars in the Hertzsprung-Russell Diagram, IAU 3rd Colloquium on Variable Stars, ed. W. Strohmeier (Kl. Veröff. Bamberg 40, No. 40), p. 36, 1965VeBam..27...36B
Bianchi, L., Shiao, B., & Thilker, D. 2017, ApJS, 230, 24, 2017ApJS..230...24B
Bradstreet, D. H., & Steelman, D. P. 2004, Binary Maker 3 Light Curve Synthesis Program. Norristown. Contact Software, 19041, 2002AAS...201.7502B
Brown, A. G. A., et al. 2018, A&A, 616, A1, 2018A&A...616A...1G
Buccino, A. P., & Mauas, P. J. 2009, A&A, 495, 287, 2009A&A...495..287B
Csizmadia, S., & Klagyivik, P. 2004, A&A, 426, 1001, 2004A&A...426.1001C
Djorgovski, S. G., et al. 2011, arXiv:1102.5004, 2011arXiv1102.5004D
Hall, D. S. 1976, The RS CVn binaries and binaries with similar properties. In International Astronomical Union Colloquium (Vol. 29, pp. 287-348). Cambridge University Press. https://doi.org/10.1017/S0252921100062011
Hall, D. S. 1991, Learning about Stellar Dynamos from Long–term Photometry of Starspots. In International Astronomical Union Colloquium (Vol. 130, pp. 353-369). Cambridge University Press. https://doi.org/10.1017/S0252921100079914
Henden, A. A., et al. 2016, VizieR Online Data Catalog: AAVSO Photometric All Sky Survey (APASS) DR9, VizieR Online Data Catalog, 2336, 2016yCat.2336....0H
Kochanek, C.S., et al. 2017, PASP, 129, p.104502. https://doi.org/10.1088/1538-3873/aa80d9
Kozhevnikova, A. V., & Alekseev, I. Y. 2015, Astronomy Reports, 59, 937, https://doi.org/10.1134/S1063772915100030
Li, L., Han, Z., & Zhang, F. 2004, MNRAS, 355, 1383, 2004MNRAS.351..137L
Main Sequence Software, 2021, Sequence Generator Pro - SGP, available from https://www.sequencegeneratorpro.com/ Accessed 15 December 2021.
Mamajek, E. 2019, "A Modern Mean Dwarf Stellar Color and Effective Temperature Sequence" available from http://www.pas.rochester.edu/~emamajek/EEM_dwarf_UBVIJHK_colors_Teff.txt Accessed March 2021.
Miyashita, K. 2007, Half Flux Diameter -Applicate to determination for faint star event, available from https://astro-limovie.info/occultation_observation/halffluxdiameter/halffluxdiameter_en.html Accessed 15 December, 2021.
Monesinos B., et al. 1998, MNRAS, 232, 361, 1988MNRAS.232..361M
Mullan, D. J. 1975, ApJ, 198, 563, 1975ApJ...198..563M
NASA/IPAC Extragalactic Database - NED, 2015, Coordinate Transformation and Galactic Extinction Calculator. Available from https://ned.ipac.caltech.edu/forms/calculator.html Accessed 20 November 2021.
Nelson, R.H. 2006, 'Minima' Software available at https://www.variablestarssouth.org/software-by-bob-nelson/ Accessed 17 July 2021.
O'Connell, D. J. K. 1951, MNRAS, 111, 642, 1951MNRAS.111..642O
Paunzen, E., & Vanmunster, T. 2016, Astronomische Nachrichten, 337, 239, 2016AN....337..239P
Pecaut, M. J., & Mamajek, E. E., 2013, ApJS, 208, 9, 2013ApJS..208....9P
Pojmański, G. 2001, The All Sky Automated Survey (ASAS-3) System–Its Operation and Preliminary Data. In International Astronomical Union Colloquium (Vol. 183, pp. 53-58). Cambridge University Press. https://doi.org/10.1017/S025292110007860X
Qian, S. B., et al. 2014. ApJS, 212, 4, 2014ApJS..212....4Q
Rhombs, C. G., & Fix, J, D. 1976, Acta Astr., 26, 301, 1976AcA....26..301R

DOI: 10.5817/OEJV2022-0231

Schlafly, E. F., & Finkbeiner, D. P. 2011, ApJ, 737, 103, 2011ApJ...737..103S
Skumanich, A. 1972, ApJ, 171, 565, 1972ApJ...171..565S
Steenwyk, S. D., Van Noord, D. M., & Molnar, L. A. 2013, arXiv:1310.0537, 2013arXiv1310.0537S
Stellingwerf, R. F. 1978, ApJ, 224, 953, 1978ApJ...224..953S
Sterken, C., & Carlos J., eds 2005, Light curves of variable stars: a pictorial atlas. Cambridge University Press, 1996lcvs.book.....S
Terrell, D., Mukherjee, J., & Wilson, R. E. 1992,. Binary stars. A pictorial atlas. Malabar: Krieger, 1992bspa.book.....T
Watson, C., Henden, A. A., & Price, A. 2010, AAVSO International Variable Star Index VSX, VizieR Online Data Catalog, 1, 2015yCat....102027W
Woźniak, P. R., et al. 2004. AJ, 127, 2436, 2004AJ....127.2436W